International Journal on
"Technical and Physical Problems of Engineering"
(IJTPE)
Published by International Organization of IOTPE

ISSN 2077-3528
IJTPE Journal
www.iotpe.com
ijtpe@iotpe.com

June 2024 | Issue 59 | Volume 16 | Number 2 | Pages 331-341

STUDY OF GEOMAGNETIC ACTIVITY ACCORDING TO KP INDEX AND ITS VARIABILITY IN RELATION TO SUNSPOTS OVER THE LAST FIVE SOLAR CYCLES

B. Chafik M. El Malki F. Miskane H. Nebdi

Laboratory of Innovation in Science, Technology and Modeling (LISTM), Faculty of Sciences, Chouaib Doukkali University, El Jadida, Morocco
chafik.b@ucd.ac.ma, elmalki.med@ucd.ac.ma, fmiskane@gmail.com, nebdi_hamid@yahoo.fr

Abstract- Solar activity refers to all changes in magnetic field and the atmosphere of the Sun. These changes are the result of the internal processes of the Sun, especially the movement of plasma and magnetic fields within the Sun. Solar activity takes many forms, including solar flares (SF), sunspots (SSN), coronal mass ejections (CME) and solar wind (SW). When these phenomena occur, they disturb the magnetic field of the magnetosphere, producing geomagnetic storms of various magnitudes. In this work, we focus on the study of geomagnetic activity through the planetary index *Kp* under extreme events conditions (major and severe storms) when *Kp* is greater than or equal to 7. During these extreme events, the earth's environment and our technology in space and land are impacted by geomagnetic disturbances. To avoid potential risks to technologies when extreme events occur, a statistical analysis is done, by using a big data of *Kp* index and extracting the very geomagnetic active days (VGAD) during the last five solar cycles (20th, 21st, 22nd, 23rd and 24th). The evolution of the monthly probabilities of occurrence during these solar cycles shows that these probabilities are higher during the months of April, May, September, and October. Our study also reveals that the majority of VGAD are observed in the descending phase of the 20th, 21st and 24th solar cycles, while their distribution is greatest in the maximum phase during the 22nd and 24th solar cycles. This study also highlights a significant correlation between the *Kp* index and SSN. However, we note that some VGAD are observed on sun spotless days.

Keywords: Geomagnetic Activity, Solar Cycle, *Kp* Index, Ionosphere, Sunspots, Extreme Events.

1. INTRODUCTION

The main source of energy on earth is the Sun, which makes life on our planet possible thanks to the sun's electromagnetic radiation. In addition, spontaneous exchanges of the quantity of energy received on earth have a direct influence on the global and local climate, and sometimes disturbs the state of the atmosphere due to several factors. The Sun constantly emits tons of matter, through electrified particles and CME. This outflow is known as the solar wind, which interacts with the Earth's environment, generating a range of disturbances that affect modern technologies such as GPS systems, power grids, telecommunications, satellites and navigation systems [1-4]. Ones of these disturbances are the geomagnetic storm.

In a previous work, a study concludes that strong geomagnetic activity is a contributing factor to US power grid disturbances [5]. Our modern society is highly susceptible to the effects of geomagnetic activity. One of their most significant phenomena is the scintillation of trans-ionospheric radio signals. This scintillation can severely degrade satellite-based communication and navigation systems [6, 7]. In addition, geomagnetic storms can have a significant impact on GPS systems, causing errors in positioning, signal loss, and outages. The severity of the impact depends on the strength of the geomagnetic storm and the location of the GPS receiver. A previous study found that GPS positioning errors were strongly correlated with the *Kp* index during a geomagnetic storm in 2015. The study found that the positioning errors increased significantly as the *Kp* index increased [7, 8]. The ionospheric disturbances caused by geomagnetic storms significantly impacted the performance of global navigation satellite system (GNSS) during geomagnetic storms period [8, 9].

Geomagnetic activity affects aeronautical radionavigation. A study of strong solar radio bursts observed reveals that air traffic radar systems are affected by strong geomagnetic activity [4]. The solar wind is a flow of charged particles (primarily protons and electrons) that emanates from the solar corona, the Sun's outer atmosphere, called the corona. This constant flow of particles propagates throughout the solar system at high speeds [2, 10]. These particles are ejected from the Sun thanks to the high temperature and pressure present in the solar corona. They travel through interplanetary space, interacting with the magnetic fields of planets and other celestial bodies along the way [10].

The solar wind has a major effect on the space environment, on Earth's ionosphere and planetary magnetospheres, triggering polar aurora and playing an

Registered: 231204 | Article Info: 1816 | Accepted: 240520
Reserved: 240414 | Available: 240630

important role in eroding the atmospheres of planets lacking a protective magnetic field [2], [11-13].

Geomagnetic activity depends on solar activity, which varies all the time. The solar cycle is a period of time during which solar activity reproduces the same behavior. To better describe geomagnetic activity, several indices have been defined: the *K* index measures the local intensity of disturbances to the horizontal components of the magnetic field over a 3-hour period, expressed on a scale from 0 to 9. Each observatory measures its local *K* index. The solar cycle's minimum and maximum intensity phases have distinct impacts on geomagnetic activity. Have different effects on geomagnetic activity. During periods of high solar activity, with a large number of sunspots and solar flares, geomagnetic storms are more frequent. On the other hand, during periods of low solar activity, geomagnetic storms are less common [2]. To our knowledge, no study using this method has ever been performed, which makes our work authentic.

In the next section (materials and methods), we explain how we extracted and processed the data to determine the VGAD, we give the equations used to calculate probabilities, correlations and statistical indicators. In the results and discussions section, we analyze, discuss, and interpret the results of our study. A conclusion summarizing the results and perspectives of our study is given.

2. MATERIALS AND METHODS

The Earth's geomagnetic activity is closely related to solar activity and varies according to solar cycles. Solar activity fluctuates periodically on a cycle averaging around 11 years, known as the solar cycle. The 11-year solar cycle was first determined by German amateur astronomer Heinrich Schwabe in 1843 [14].

Table 1. Periods of various solar cycles [16]

Cycle no.	Start	End	Duration
1	August 1755	March 1766	11.3
2	1766	1775	9
3	1775	1784	9
4	1784	1798	14
5	1798	1810	12
6	1810	1823	13
7	1823	1833	10
8	1833	1843	10
9	1843	1855	12
10	1855	1867	12
11	1867	1878	11
12	1878	1890	12
13	1890	1902	12
14	1902	1913	11
15	1913	1923	10
16	1923	1933	10
17	1933	1944	11
18	1944	1954	10
19	1954	1964	10
20	October 1964	May 1976	12
21	Jun 1976	Aug 1986	10
22	September 1986	May 1996	10
23	May 1996	December 2007	11.6
24	January 2008	Mars 2019	11.3
25	April 2019	Estimated around 2031	-

In 1849, Swiss astronomer Johann Rudolf Wolf established a method for calculating solar activity based on the number of sunspots. Schwabe's cycles are numbered from the maximum of 1761 [15]. Table 1 defines the periods of the various solar cycles [16]. In this work, we exploit the database of GFZ, which gives the value of the *Kp* index with a time step of three hours. These data are processed to determine the VGAD, characterized by a *Kp* value greater than or equal to 7 recorded at least once during the 8 measurements per day. The evolution of the VGAD over the last five solar cycles (20th, 21st, 22nd, 23rd, and 24th cycle) is then determined. The monthly probability of occurrence of these days during each cycle is used to calculate correlations [17]. Geomagnetic storms can be related to the *Kp* index [18]. Table 2 classifies the intensity of these storms according to the *Kp* index [19]. It indicates the level of disturbance caused to the Earth's magnetic field by the interaction between this field and the solar wind.

Table 2. Scale of *Kp* index [19]

Kp index	Signification
0, 1, 2	calm
3	unsettled
4	active
5	minor storm
6	moderate storm
7	major storm
8, 9	severe storm

Eight terrestrial magnetometers distributed around the globe are used by NOAA's Space Weather Prediction Center to calculate the estimated 3-hour *Kp* index. SWPC and data providers from over the world, including the British Geological Survey (BGS), Natural Resources Canada (NRCAN), the U.S. Geological survey (USGS), Geoscience Australia (GA), and the German Research Centre for Geosciences (GFZ) have collaborated to provide these data and make it accessible. The Korean Space Weather Center and the Institute de Physique du Globe de Paris also provide significant magneto metric observations. The *K* index alerts are emitted when *Kp* indices are reached 4 or more [20].

In previous studies of the variation of the *K* index have shown that strong ionospheric turbulence is 100% manifested when the *K* index is greater than or equal to 7 [13], [22]. On days when a *K* value greater than or equal to 7 is recorded, the day is considered to be one of the VGAD. In this article, we will study only the VGAD but for $Kp \geq 7$ in order to obtain a global idea about correlation between the previously mentioned indices and the last five solar cycles, and finally we will focus on a new in-depth view between these parameters and compare them with the observed sunspots to interpret the results obtained.

We also use the database extracted from the Royal Observatory of Belgium (Brussels) for daily sunspot data. [23]. To investigate the relationship between sunspots and very geomagnetic active days number (VGADN), data were collected over a 55-year period (5 solar cycles), from 1964 to 2019. We analyzed the data using statistical techniques to determine the correlation between sunspots and the *Kp* geomagnetic index. Our study covered five solar cycles from 01/10/1964 to 31/03/2019.

To study the reliability of the proposed model, the use of statistical indicators is essential. In fact, there are several indicators in the literature, in the present work we have chosen the most used by researchers to investigate the performance of the proposed model such MBE, RMSE, nRMSE, TS, SD and Pearson's correlation coefficient (ρ) [24, 25].

The model error is a term used to define the difference between the measured and the predicted values as follows:

$$e_{xi} = x_{meas_i} - x_{pred_i} \quad (1)$$

where, x_{meas_i} and x_{pred_i} denote the ith measured and predicted value, respectively. The error's arithmetic mean is represented by the MBE. The predicted data is overestimated by a positive MBE, while the measured value is underestimated by a negative MBE [26, 27]:

$$MBE = \frac{1}{N}\sum_{i=1}^{N} e_{xi} \quad (2)$$

where, N represents the sum of observations in the dataset. The short-term performance of a predicted dataset can be evaluated by the RMSE. Zero is the ideal value for this indicator, which is always positive [24, 27]:

$$RMSE = \sqrt{\frac{1}{N}\sum_{i=1}^{N} e_{xi}^{\,2}} \quad (3)$$

Comparing prediction models becomes easier with the use of standard performance evaluation techniques. The quality of the prediction model is more accurately evaluated by the normalized root mean square error (nRMSE) than by the RMSE or MBE [24, 26, 27].

$$nRMSE = \left(\frac{1}{N}\sum_{i=1}^{N}\frac{e_{xi}}{x_{meas_i}}\right)\times 100 \quad (4)$$

TS is a test that is commonly used to determine if a prediction model is considerably different from the measured data or not. The predicted data will be more accurate if the TS value is smaller [27]:

$$TS = \sqrt{\frac{(N-1)MBE^2}{RMSE^2 - MBE^2}} \quad (5)$$

The standard deviation is a measure of the difference between measured and predicted data. Zero is the ideal value for standard deviation which is always positive [27]:

$$SD = \sqrt{\frac{N\left(RMSE^2 - MBE^2\right)}{(N-1)}} \quad (6)$$

The Pearson correlation coefficient (ρ) is used to evaluate the Pearson criterion. If 2 datasets X and Y are strongly correlated, the Pearson coefficient will be -1 (inverse correlation) or 1 (direct correlation). On the other hand, a zero or weak correlation can be concluded when the Pearson coefficient is approaching zero [27]:

$$\rho = \frac{\sum_{i=1}^{n}\left(X_i - \bar{X}\right)\left(Y_i - \bar{Y}\right)}{\sqrt{\sum_{i=1}^{n}\left(X_i - \bar{X}\right)^2}\sqrt{\sum_{i=1}^{n}\left(Y_i - \bar{Y}\right)^2}} \quad (7)$$

3. RESULTS AND DISCUSSIONS

In this section, we make a comparison of the different results obtained previously and we use the different mathematical methods to study the reliability of the experimental results. Figure 1 shows the evolution of VGADN over the last five solar cycles. The evolution of the VGADN shows an increase in the number of days at the beginning of each cycle, and a decrease in the number of days at the end of each one. The number of VGAD over the last five solar cycles increases cycle by cycle, reaching an absolute maximum at the 22nd cycle, and then decreases cycle by cycle. In total, 377 VGAD of 1905 days were identified, representing a percentage of 1.89%.

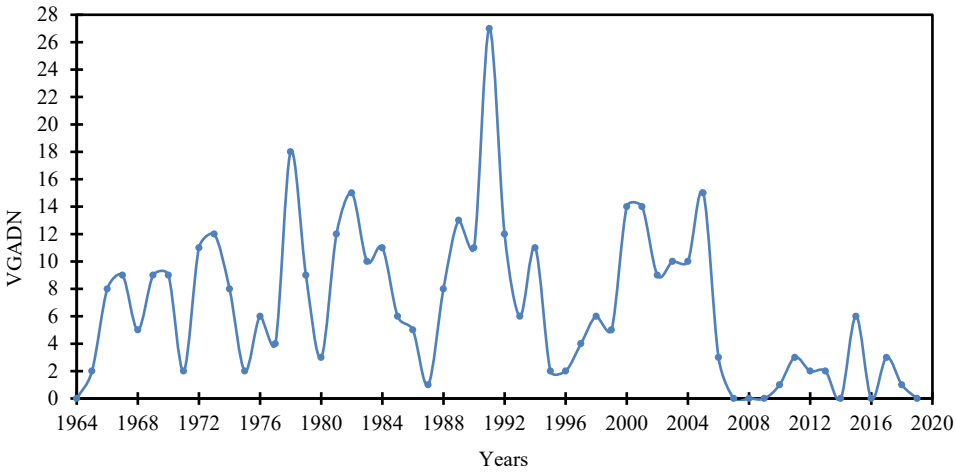

Figure 1. Evolution of the very geomagnetic active days over the last 5 solar cycles

We have determined the maximum VGAD numbers during each solar cycle. Figure 2 shows the evolution of these maxima during last five solar cycles. The maximum of the VGAD differs from one cycle to other according to several factors, including solar activity. One of the most significant indices of this activity is the number of sunspots observed. This evolution takes the form of a long 55-year cycle, with a maximum at the 22nd cycle and two minima at the 20th and 24th solar cycles. Figures 3-7 show the evolution of the occurrence of VGAD during each solar cycle of last five solar cycles.

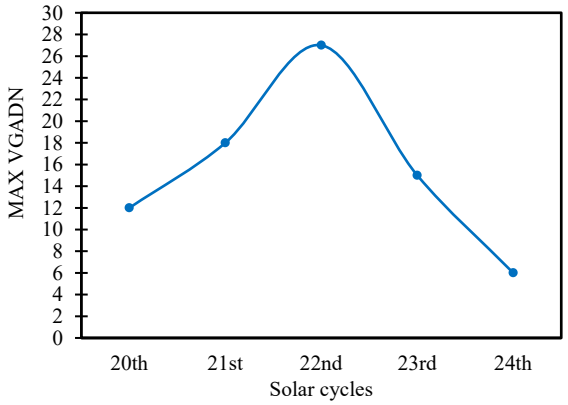

Figure 2. Evolution of maximum VGADN during the 20th, 21st, 22nd, 23rd and 24th solar cycles

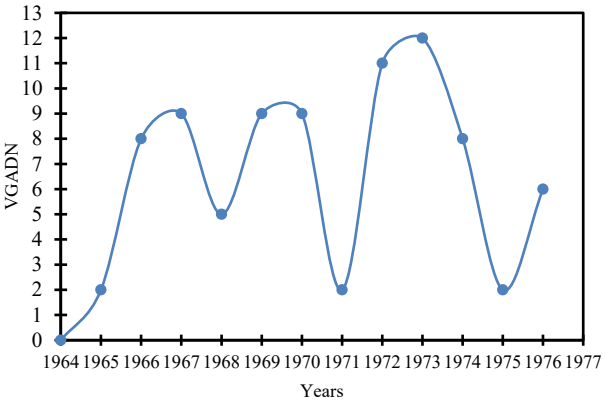

Figure 3. Evolution of the very geomagnetic active days during the 20th cycle

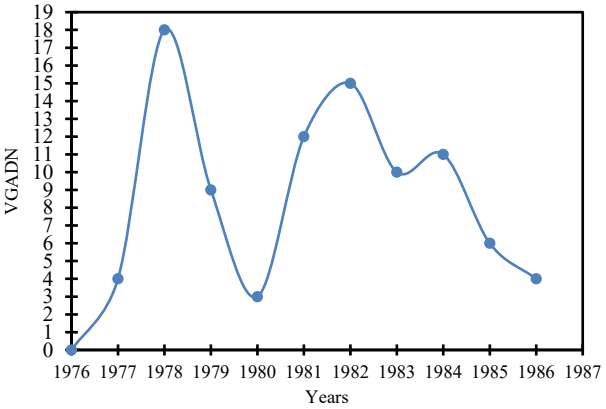

Figure 4. Evolution of the very geomagnetic active days during the 21st cycle

Figures 3-7 show that VGADN fluctuates between the two minima of each solar cycle, but the general behavior is similar. To look for seasonal dependence, we calculated the monthly probabilities of occurrence on VGAD defined by the following procedure.

The probability of month X in a cycle is defined by the ratio between the (VGADNM) of very geomagnetic active days number during this month in the entire solar cycle and the sum of very geomagnetic active days in the solar cycle, and write it as:

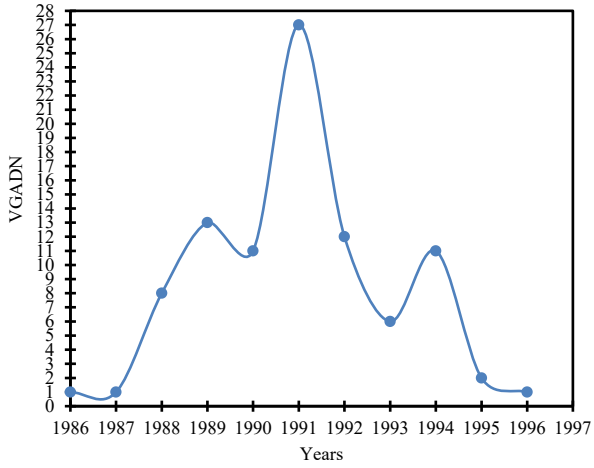

Figure 5. Evolution of very geomagnetic active days during the 22nd cycle

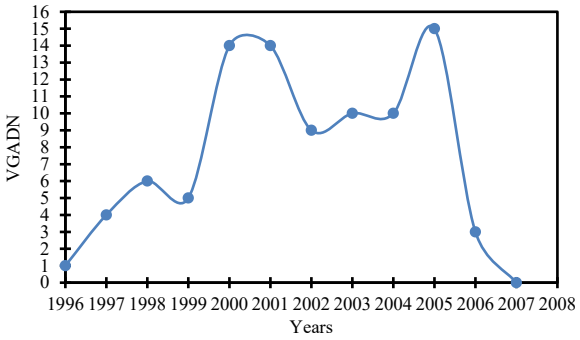

Figure 6. Evolution of the very geomagnetic activity days during the 23rd cycle

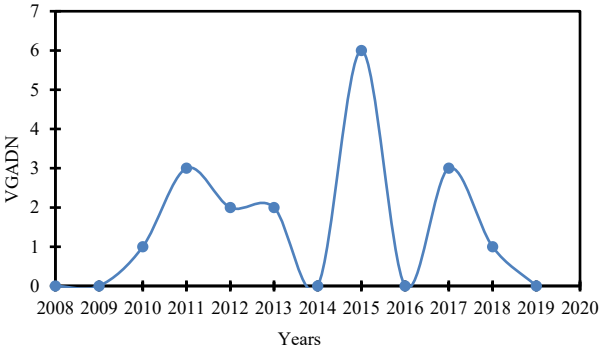

Figure 7. Evolution of the very geomagnetic activity days during the 24th cycle

$$P(X)=\frac{VGADNM(X)}{VGADNC(Y)} \tag{8}$$

where, X=1, 2, 3, …12 and Y=20, 21, 22, 23 and 24.

During the 20th solar cycle, we counted 83 VGAD. Figure 8 shows the monthly probabilities of occurrence of the VGAD during the 20th solar cycle.

During the 21st solar cycle, we counted 92 very geomagnetic activity days. Figure 9 shows the monthly probabilities of occurrence of the VGAD during the 21st solar cycle.

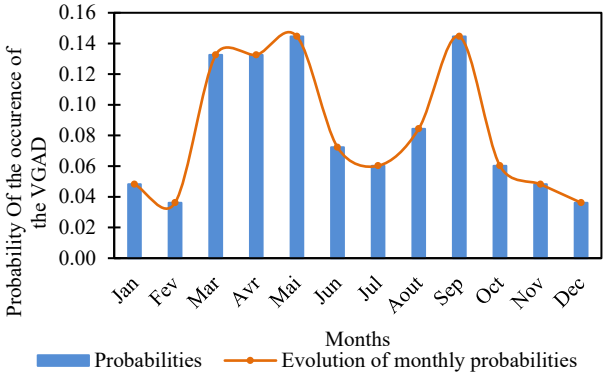

Figure 8. Probability of monthly occurrence of the very geomagnetic active days during the 20th solar cycle

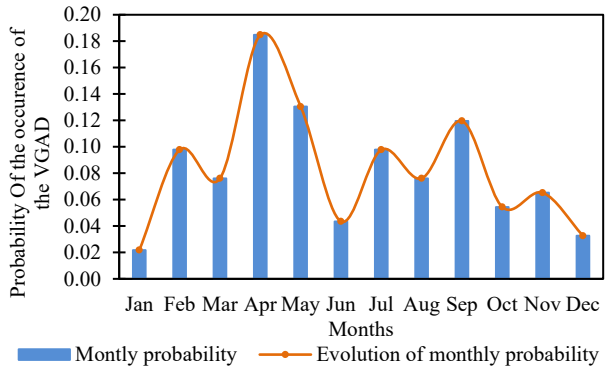

Figure 9. Probability of monthly occurrence of the very geomagnetic active days during the 21st solar cycle

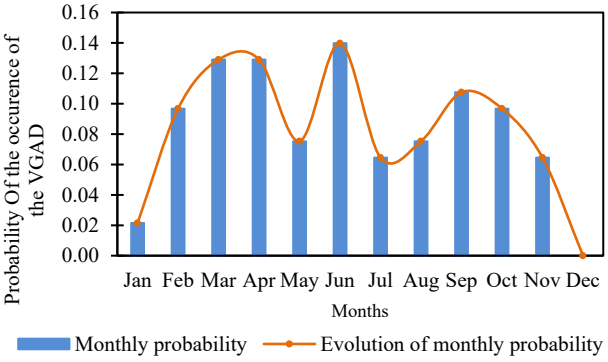

Figure 10. Probability of monthly occurrence of the very geomagnetic active days during the 22nd solar cycle

During the 22nd solar cycle, we counted 93 VGAD. Figure 10 shows the monthly probabilities of occurrence of VGAD during the 22nd solar cycle.

During the 23rd solar cycle, we counted 91 VGAD. Figure 11 shows the monthly probabilities of occurrence of VGAD during the 23rd solar cycle.

During the 24th solar cycle, we counted 18 VGAD. Figure 12 shows the monthly probabilities of occurrence of VGAD during the 24th solar cycle.

Using the previously defined law, correlations are calculated between the monthly probabilities of occurrence of VGAD in pairs of solar cycles, and the correlations between the monthly probabilities of occurrence of VGAD in each solar cycle and those in all five solar cycles. Table 3 shows the correlations calculated.

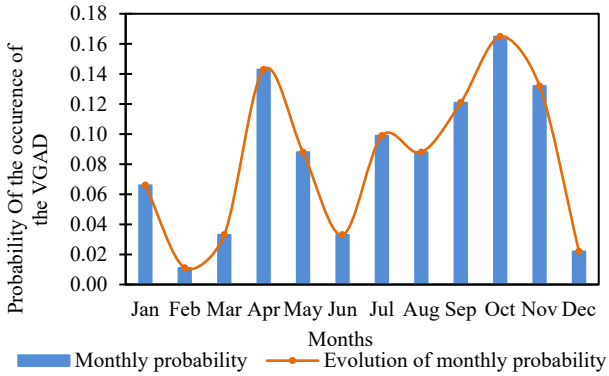

Figure 11. Probability of monthly occurrence of the very geomagnetic active days during the 23rd solar cycle

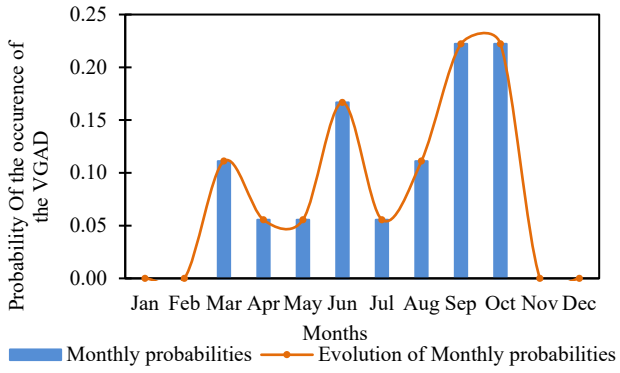

Figure 12. Probability of monthly occurrence of the very geomagnetic active days during the 24th solar cycle

Table 3. Correlation between monthly appearance probabilities of solar cycle pairs

	20th cycle	21st cycle	22nd cycle	23rd cycle	24th cycle
20th cycle					
21st cycle	0.685				
22nd cycle	0.550	0.487			
23rd cycle	0.271	0.389	0.147		
24th cycle	0.430	0.057	0.587	0.370	
All 5 cycles	0.810	0.806	0.732	0.644	0.561

The correlations between the probabilities of occurrence of the VGAD between a pair of solar cycles are low (0.43; 0.06; 0.59; 0.37; 0.27; 0.39; 0.15; 0.55; 0.49; 0.68). But the correlations between the probabilities of occurrence of VGAD during the 5 cycles and each of these cycles is strong, with the following values: 0.81; 0.81; 0.73; 0.64; 0.56 for 20th, 21st, 22nd, 23rd and 24th respectively. And this means that more we have data more we can study the VGAD.

In order to develop an empirical model that determines the evolution of the monthly probabilities of the occurrence of VGA days, we first calculate the monthly probabilities of the occurrence of the VGAD during the last five solar cycles. We do this by taking the ratio of the VGADNM during the last five cycles to the sum of VGAD during all months in the last five solar cycles. Figure 13 shows the monthly probabilities of the occurrence of the VGAD during last five solar cycles.

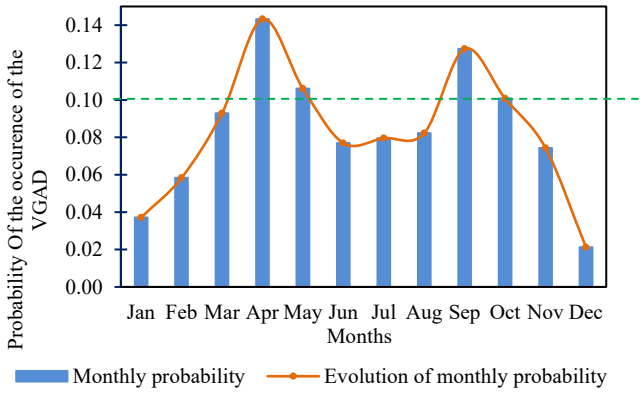

Figure 13. Probability of monthly occurrence of the very geomagnetic active days during the 20th, 21st, 22nd, 23rd and 24th solar cycles

We can see that the probabilities for April, May, September, and October exceed 0.10, reaching 0.14 for April, 0.10 for May, 0.13 for September, and 0.10 for October. To have an idea about the evolution of monthly probability of the occurrence of the VGA days for these months as a function of each solar cycle, a polynomial regression model of order 4 then performed to determine a model for calculating the probabilities of these months. We have plotted Figures 14-17.

From the evolution of the monthly probabilities of the most active months (April, May, September, and October) during the last five solar cycles, we determined the equations which describe these evolutions by the polynomial model, and then we made the regression by this model. The probabilities smoothed $P_m(x)$ of month x by this model follow the Equation (9):

$$P_m(X) = a_0 + a_1 x + a_2 x^2 + a_3 x^3 + a_4 x^4 \quad (9)$$

where, x=1, 2, 3, 4 and 5 for 20th, 21st, 22nd, 23rd and 24th solar cycles respectively. Table 4 gives the coefficients a_i used to calculate the probabilities for the months in question.

Table 4. Smoothed coefficient a_i

Months	Coefficients a_i				
	a_0	a_1	a_2	a_3	a_4
April	–0.5536	1.2654	–0.7395	0.1747	–0.0145
May	–0.2128	0.7087	–0.4526	0.1105	–0.0092
September	0.2203	–0.1263	0.0673	–0.0188	0.0021
October	0.1235	–0.0916	0.027	0.0019	–0.0006

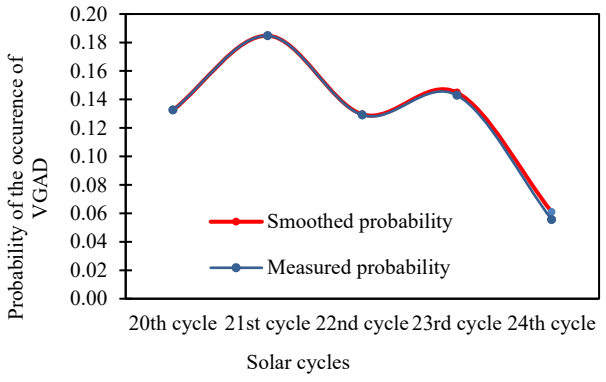

Figure 14. Evolution of the probability of the occurrence of very geomagnetic days in April during last five solar cycles

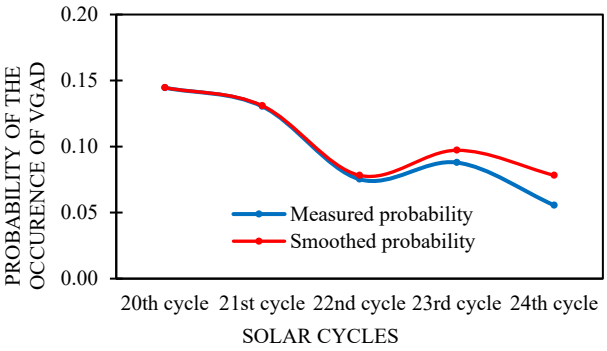

Figure 15. Evolution of the probability of the occurrence of very geomagnetic days in May during the last five solar cycles

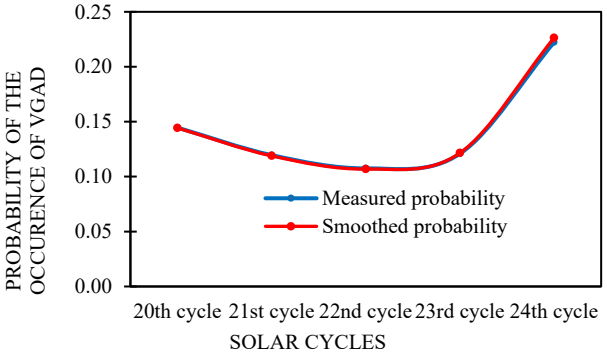

Figure 16. Evolution of the probability of the occurrence of very geomagnetic days in September during the last 5 solar cycles

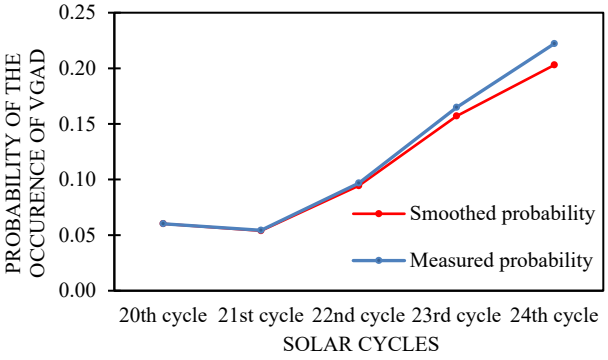

Figure 17. Evolution of the probability of the occurrence of very geomagnetic days in October during the last 5 solar cycles

Table 5 gives the different statistical indicators defined previously for a study of the reliability of the models developed.

Table 5. summary of statistical indicators

	April	May	September	October	Average
MBE	–0.002	–0.007	0.056	0.006	0.013
RMSE	0.003	0.011	0.115	0.009	0.034
NRMSE	–2.266	–11.134	2.901	3.338	–1.790
TS	1.527	1.679	1.131	1.663	1.500
SD	0.002	0.009	0.112	0.008	0.033

We can see that the regression model for each month gives a good correlation between the measured probabilities and the smoothed probabilities. We conclude that the probabilities of the occurrence of the VGAD do not follow a single law, so a simple model is not sufficient.

Therefore, it is necessary to use other statistical or more generally mathematical methods to perform this modelling. Concerning the exploitation of daily sunspots extracted from the mentioned database with the objective of finding a relationship between sunspots and *Kp* geomagnetic indices, we have plotted the evolution of SSN and the VGAD (*Kp*=7, 8 or 9) as a function of date in four phases to obtain the following graphs (Figures 20-25).

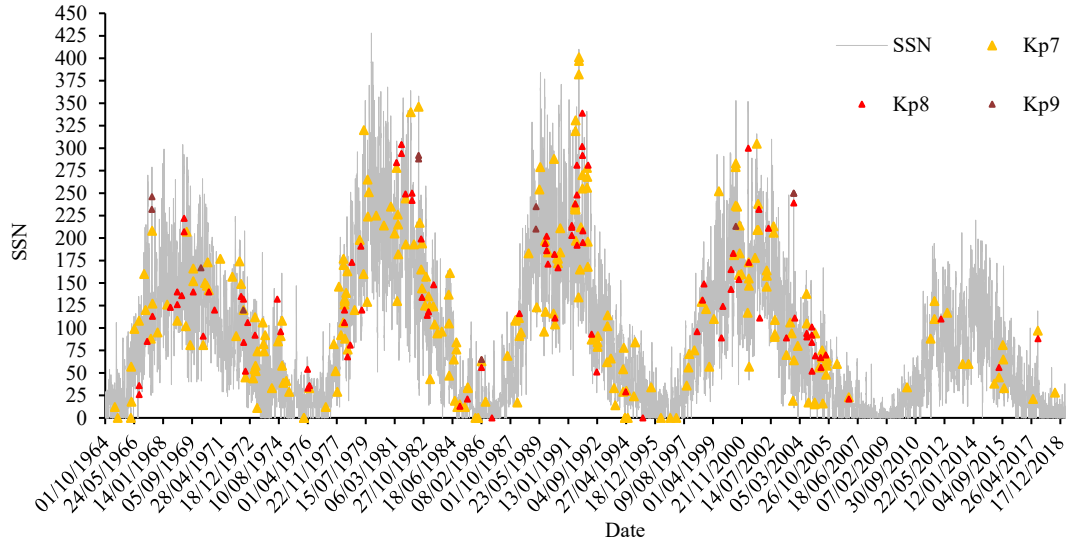

Figure 18. Evolution of SSN and distribution of SSN for VGAD during the last 5 solar cycles

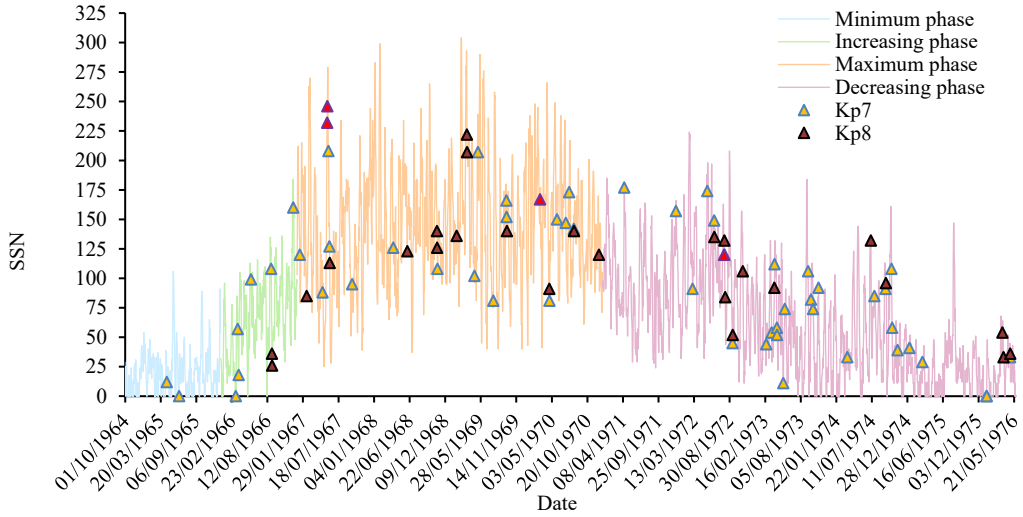

Figure 19. Evolution of SSN and distribution of SSN for VGAD during the 20th solar cycle

Figure 18 shows that the distribution of VGAD over the last 5 solar cycles constructs a large cycle composed of 5 phases: first minimum phase (20th cycle), increasing phase (21st cycle), maximum phase (22nd cycle), descending phase (23rd cycle) and second minimum (cycle). On the other hand, we note that the geomagnetic activity represented by the *Kp* index depends on the solar activity represented by the Sunspots. In the descending phase of the SSN evolution curve during the 20th cycle, we count 41 VGAD, which represents 49.40% of the VGAD observed during the cycle. In the descending phase of the SSN evolution curve during the 21st cycle, we count 46 VGAD, which represents 50% of the VGAD counted during the cycle.

In the descending phase of the SSN evolution curve during the 22nd cycle, we count 32 VGAD, which represents 24.41% of the VGAD observed during the cycle. In the descending phase of the SSN evolution curve during the 23rd cycle, we count 38 VGAD, which represents 41.76% of the VGAD observed during the cycle.

In the descending phase of the SSN evolution curve during the 24th cycle, we count 10 VGAD, which represents 55.56% of the VGAD observed during the cycle. Table 6 summarizes the number and the percentage of VGAD during the four phases of each cycle [16, 28].

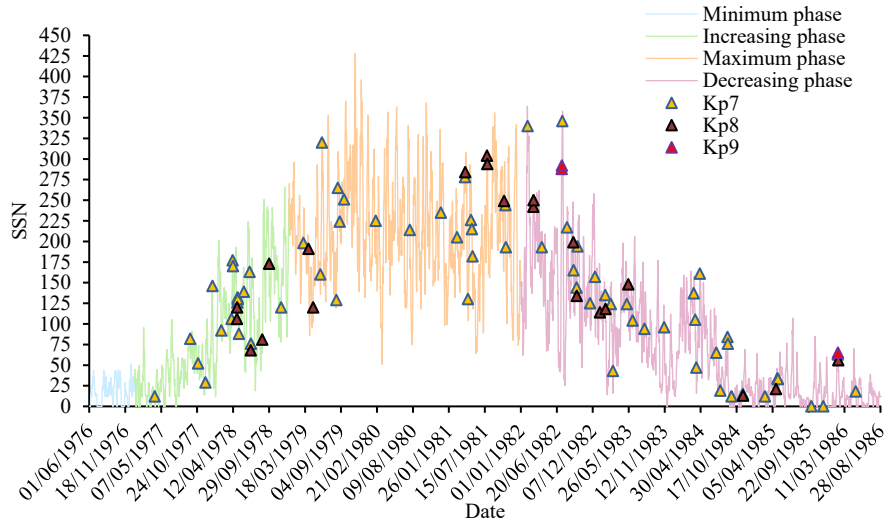

Figure 20. Evolution of SSN and distribution of SSN for VGAD during 21st solar cycle

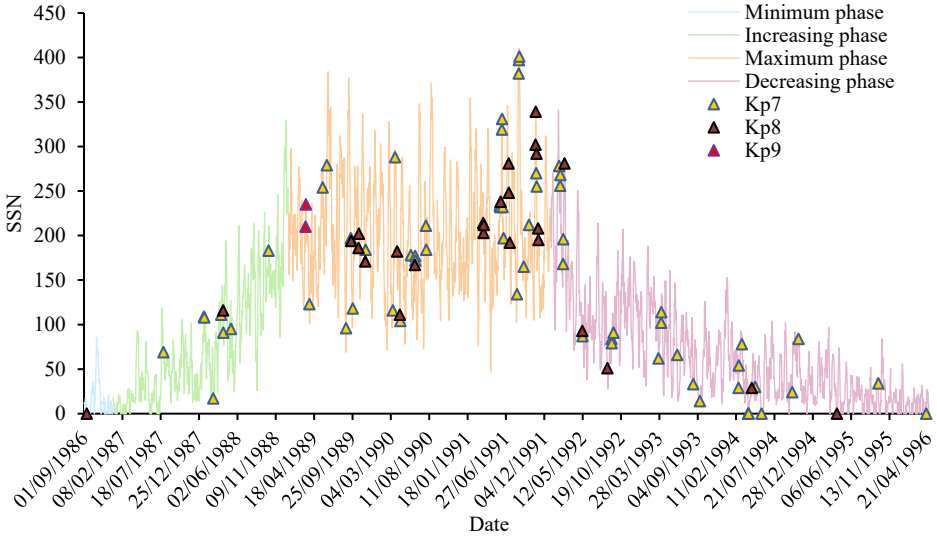

Figure 21. Evolution of SSN and distribution of SSN for VGAD during the 22nd solar cycle

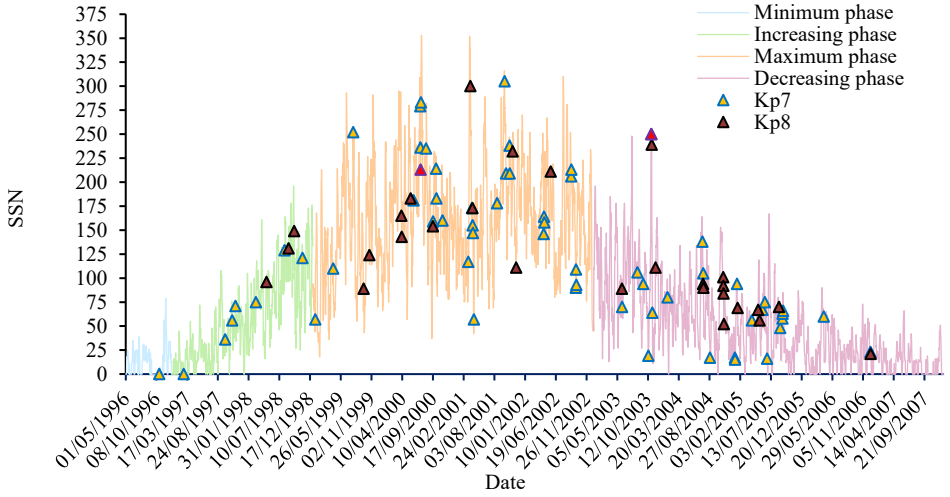

Figure 22. Evolution of SSN and distribution of SSN for VGAD during the 23rd solar cycle

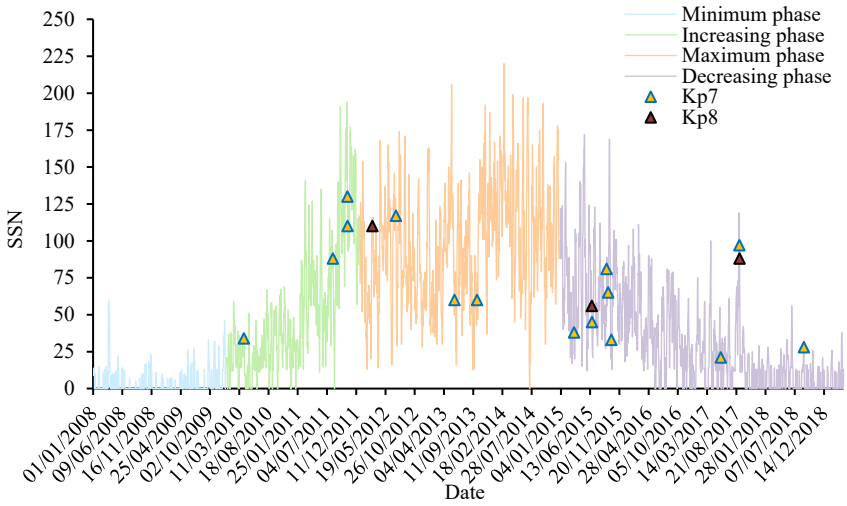

Figure 23. Evolution of SSN and distribution of SSN for VGAD during the 24th solar cycle

Table 6. Summary of number and percentage of VGAD during phases of last five solar cycles

Solar cycle	Phase	Phase duration (years)	VGAD number	Percentage %
20th	Minimum	2	2	2.41
	Increasing	1	8	9.64
	Maximum	4	32	38.55
	Decreasing	5	41	49.40
21st	Minimum	1	0	0
	Increasing	2	22	23.91
	Maximum	3	24	26.09
	Decreasing	4	46	50
22nd	Minimum	1	1	1.08
	Increasing	2	9	9.68
	Maximum	4	51	54.84
	Decreasing	4	32	34.41
23rd	Minimum	1	1	1.10
	Increasing	2	10	10.99
	Maximum	4	42	46.15
	Decreasing	4	38	41.76
24th	Minimum	2	0	0
	Increasing	2	4	22.22
	Maximum	3	4	22.22
	Decreasing	4	10	55.56

From the Figures 18, 19, 20, 21, 22 and 23, we can see that the number of VGAD during 20th, 21st and 24th solar cycles is greatest in the descending phases, while the distribution of VGAD is greatest in the maximum phase during the 22nd and 24th solar cycles. This result confirms that in the descending phase of the cycle, geomagnetic activity is more remarkable, and in this period more extreme space weather events can take place.

4. CONCLUSION AND PERSPECTIVES

The earth continuously receives provident electromagnetic radiation from the sun at all times, and during this study we were able to show that the disturbance of geomagnetic activity expressed by the *Kp* geomagnetic index is directly caused by solar activity, more precisely sunspot fluctuations. Our study revealed significant correlations between variations in *Kp* index and different phases of the solar cycle. In general, the monthly probabilities of occurrence of VGAD in April, May, September, and October are highest. We can conclude that the number of VGAD during 20th, 21st and 24th solar cycles is very important in the descending phases, but the distribution of VGAD is greatest in the maximum phase during the 22nd and 24th solar cycles, when extreme space weather events can be more observed.

These results underline the importance of understanding the impact of solar variations on the Earth's magnetic field, particularly their effects on technologies sensitive to geomagnetic disturbances such as power grids, global navigation satellite systems (Galileo, GPS, Beidou, Glonass, …), satellite communications, military and civil aviation, astronauts, pilots on high-altitude flights. This work will enable us to better anticipate and mitigate the potential effects of geomagnetic variations induced by solar activity, paving the way for significant advances in the protection of human activities and our technological infrastructures, against these natural catastrophe's phenomena.

ACKNOWLEDGEMENTS

The authors would like to thank the GFZ institute and the Royal Observatory of Belgium for making their usable databases available to us and to all researchers on their website.

NOMENCLATURES

1. Acronyms

MBE	Mean Bias Error
nRMSE	Normalized Root Mean Square Error
RMSE	Root Mean Square Error
SD	Standard Deviation
TS	Test Statistic
VGAD	Very geomagnetic active days
VGADNC	Very geomagnetic active days number in the cycle
VGADNM	Very geomagnetic active days number in the month
NRCAN	Natural Resources Canada
GFZ	German Research Centre for Geosciences

2. Symbols / Parameters

ρ: Pearson's correlation coefficient
e_{xi}: Model error
N: Total number of the measurements in the dataset
SNN: Sunspot Number
K: Local geomagnetic index
Kp: Planetary geomagnetic index

REFERENCES

[1] H. Nebdi, "Space Weather and Link to Climate Change", Handbook of Research on Global Environmental Changes and Human Health, IGI Global, pp. 1-20, 2019.

[2] E.N. Parker, "Dynamics of The Interplanetary Gas and Magnetic Fields", American Astronomical Society, No. 128, pp. 664-676, 1958.

[3] S.K. Solanki, N.A. Krivova, J.D. Haigh, "Solar Irradiance Variability and Climate", Annual Review of Astronomy and Astrophysics, No. June, pp. 311-351, 2013.

[4] C. Marque, et al., "Solar Radio Emission as a Disturbance of Aeronautical Radionavigation", Journal of Space Weather and Space Climate, Vol. 8, 2018.

[5] C.J. Schrijver, S.D. Mitchell, "Disturbances in The US Electric Grid Associated with Geomagnetic Activity", Journal of Space Weather and Space Climate, Vol. 3, 2013.

[6] G. Li, B. Ning, B. Zhao, L. Liu, J. Y. Liu, K. Yumoto, "Effects of Geomagnetic Storm on GPS Ionospheric Scintillations at Sanya", J. Atmos. Sol. Terr. Phys., Vol. 70, No. 7, pp. 1034-1045, 2008.

[7] Y. Jin, W.J. Miloch, J.I. Moen, L.B.N. Clausen, "Solar Cycle and Seasonal Variations of The GPS Phase Scintillation at High Latitudes", Journal of Space Weather and Space Climate, Vol. 8, 2018.

[8] Y. Wang, et al., "Effects of Strong Geomagnetic Storms on The Ionosphere and Degradation of Precise Point Positioning Accuracy During The 25th Solar Cycle Rising Phase: A Case Study", Remote Sens, Vol. 15, No. 23, Basel, Switzerland, 2023.

[9] S. Kumar, A.K. Singh, "The Effect of Geomagnetic Storm on GPS Derived Total Electron Content (TEC) At Varanasi, India", J. Phys. Conf. Ser., Vol. 208, 2010.

[10] S.R. Cranmer, "New Views of The Solar Wind with The Lambert W Function", Am. J. Phys., Vol. 72, No. 11, pp. 1-16, 2004.

[11] C. Auntarin, P. Chunpang, C. Plybour, T. Laosuwan, "Monitoring and Analysis on Change of Land Surface Temperature Based on Satellite Data", International Journal on Technical and Physical Problems of Engineering (IJTPE), Issue 54, Vol. 15, No. 1, pp. 178-183, March 2023.

[12] H.A. Elliott, J.M. Jahn, D.J. McComas, "The *Kp* Index and Solar Wind Speed Relationship: Insights for Improving Space Weather Forecasts", Space Weather, Vol. 11, No. 6, pp. 339-349, 2013.

[13] H. Nebdi, "Study of Geomagnetic Activity During Three Solar Cycles Using a K Index Data Study of Geomagnetic Activity During Three Solar Cycles Using a K-Index Data Base", Umm Al Qura Univ. J. App. Sci., Vol. 2, No. 1, pp. 33-41, 2010.

[14] F. Clette, L. Svalgaard, J.M. Vaquero, E.W. Cliver, "Revisiting the Sunspot Number: A 400-Year Perspective on The Solar Cycle", Space Sci. Rev., Vol. 186, No. 1-4, pp. 35-103, 2014.

[15] J.A. Eddy, "The Maunder Minimum", Science (1979), Vol. 192, No. 4245, pp. 1189-1202, 1976.

[16] S. Sawadogo, D.A. Gnabahou, T. Pahima, F. Ouattara, "Solar Activity: Towards A Standard Classification of Solar Phases from Cycle 1 To Cycle 24", Advances in Space Research, Vol. 73, No. 1, pp. 1041-1049, January 2024.

[17] Helmholtz Zentrum Potsdam - Deutsches Geo Forschungs Zentrum GFZ, "Geomagnetic indices (*Kp*, ap)", Hybrid of Nowcast and Definite *Kp* and Ap Values, Simple ASCII Format, The Directory Contains Real Time Files, Files with all Values Since 1932, Year Files, and Files with Ap and Solar Activity Indices SN and F10.7, 21 December 2021, https://kp.gfz-potsdam.de/en/data.

[18] J. Bartels, N.H. Heck, H.F. Johnston, "The Three-Hour-Range Index Measuring Geomagnetic Activity", American Geophysical Union, Vol. 44, No. 4, pp. 411-454, 1938.

[19] S. Chakraborty, S.K. Morley, "Probabilistic Prediction of Geomagnetic Storms and The Kp Index", Journal of Space Weather and Space Climate, Vol. 10, 2020,

[20] NOAA Space Weather Prediction Center, "Current Space Weather Conditions: Forecasts", PLANETARY K-INDE, December 12, 2023. www.swpc.noaa.gov/products/planetary-k-index.

[21] H. Nebdi, R. Warnant, S. Lejeune, "Study of The Correlation Between Smallscale TEC Variability and Geomagnetic Activity", Technical Report of Work Package, Vol. 222, No. 16913/03, January 2004.

[22] Royal Observatory of Belgium, "Sunspot Data from the World Data Center SILSO", International Sunspot Number Monthly Bulletin and Online Catalogue, March 2023, www.sidc.be/silso/datafiles.

[23] J.A. Duffie, W.A. Beckman, "Solar Engineering of Thermal Processes", Wiley, New York, USA, 2013.

[24] S.A.M. Maleki, H. Hizam, C. Gomes, "Estimation of Hourly, Daily and Monthly Global Solar Radiation on Inclined Surfaces: Models Re-Visited", Energies, Vol. 10, No. 1, pp. 1-28, Basel, Switzerland, 2017.

[25] M. Vyas, N. Hemrajani, "Predicting Effort of Agile Software Projects Using Linear Regression, Ridge Regression and Logistic Regression", International Journal on Technical and Physical Problems of Engineering (IJTPE), Issue 47, Vol. 13, No. 2, pp. 14-19, June 2021.

[26] C. Hajjaj, et al., "Evaluation, Comparison and Experimental Validation of Different PV Power Prediction Models Under Semi-Arid Climate", Energy Convers Manag, Vol. 173, pp. 476-488, August 2018.

[27] D. Granados Lopez, A. Suarez Garcia, M. Diez Mediavilla, C. Alonso Trist, "Feature Selection for Cie Standard Sky Classification", Solar Energy, Vol. 218, pp. 95-107, March 2021.

[28] Y.I. Yermolaev, et al., "Solar Wind Parameters in Rising Phase of Solar Cycle 25", Space Research Institute, Russian Academy of Sciences, License CCBY4.0, p. 117997, Moscow, Russia, April 2023.

BIOGRAPHIES

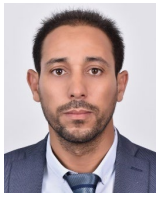

Name: **Bouchaib**
Surname: **Chafik**
Birthday: 20.12.1984
Birthplace: Sidi Bennour, Morocco
Bachelor: Renewable Energies, Faculty of Sciences, Chouaib Doukkali University, El Jadida, Morocco, 2016
Master: Materials and Radiation, Energy and Environment, Faculty of Sciences, Chouaib Doukkali University, El Jadida, Morocco, 2018
Doctorate: Student, Department of Physics, Faculty of Sciences, Chouaib Doukkali University, El Jadida, Morocco, Since 2018
Research Interests: Materials Physics, Theoretical Physics, Experimental Physics, Geophysics
Scientific Publications: 1 Paper

Name: **Mohammed**
Surname: **El Malki**
Birthday: 05.10.1991
Birthplace: Settat, Morocco
Bachelor: Renewable Energies, Faculty of Sciences, Chouaib Doukkali University, El Jadida, Morocco, 2016
Master: Materials and Radiation, Energy and Environment, Faculty of Sciences, Chouaib Doukkali University, El Jadida, Morocco, 2018
Doctorate: Student, Department of Physics, Faculty of Sciences, Chouaib Doukkali University, El Jadida, Morocco, Since 2018
Research Interests: Materials Physics, Theoretical Physics, Experimental Physics
Scientific Publications: 2 Papers

Name: **Fatiha**
Surname: **Miskane**
Birthday: 22.06.1960
Birthplace: El Jadida, Morocco
Bachelor: Physics of Materials, Department of Physics, Faculty of Sciences, Mohammed V University, Rabat, Morocco, 1985
Masters: Condensed Matter Physics, Department of Physics, Faculty of Sciences, Mohammed V University, Rabat, Morocco, 1986
Doctorate: Physics of Plasma, Department of Physics, Faculty of Science Ben M'Sik, Hassan II University, Casablanca, Morocco, 2002
The Last Scientific Position: Prof., Department of Physics, Faculty of Sciences, Chouaib Doukkali University, El Jadida, Morocco, Since 2000
Research Interests: Physics of Plasmas, Controlled Thermonuclear Fusion, Plasma of Tokamak
Scientific Publications: 9 Papers
Scientific Memberships: International Society of Muslim Women in Science (ISMWS)

Name: **Hamid**
Surname: **Nebdi**
Birthday: 01.10.1968
Birthplace: El Jadida, Morocco
Bachelor: Physics / Electronics, Department of Physics, Faculty of Sciences, Chouaib Doukkali University, El Jadida, Morocco, 1993
Master: 1- Radiation-Matter Physics, Faculty of Science Ben M'Sik, Hassan II University, Casablanca, Morocco, 1995, 2- Atomic Physics, Catholic University of Louvain, Ottignies-Louvain-la-Neuve, Belgium, 1997
Doctorate: Atomic Physics, Catholic University of Louvain, Ottignies-Louvain-la-Neuve, Belgium, 2000
The Last Scientific Position: Prof., Department of Physics, Faculty of Sciences, Chouaib Doukkali University, El Jadida, Morocco, Since 2011
Research Interests: Space Weather, Atomic and Laser Physics, Education, Innovation in Science, Technology and Modeling
Scientific Publications: 81 Papers, 5 Projects, 7 Theses
Scientific Memberships: SPANET, GIRGEA, AERDDS